Electronic Supplementary Information

Grain boundary passivation as an optimal strategy for perovskite solar cells with improved stability

Yin Li[a], *Hongbo Mo*[a], *Jingbo Wang*[a], *Zhengtian Yuan*[a], *Yanling He*[b], *Tao Zhu*[c], *Xiaoxue Fan*[d], *Gang Li*[c], *Jasminka Popović*[e] *and Aleksandra. B. Djurišić*[a,] *

[a] *Department of Physics, The University of Hong Kong, Pokfulam Road, Hong Kong SAR, China.*

[b] *Material characterization and preparation facility, The Hong Kong University of Science and Technology (Guangzhou), No.1 Duxue Road, Dongchong Town, Nansha District, Guangzhou, Guangdong Province, China*

[c] *Department of Electrical and Electronic Engineering, Research Institute for Smart Energy (RISE), The Hong Kong Polytechnic University, 11 Yuk Choi Rd, Hung Hom, Hong Kong SAR, China.*

[d] *Dept. of Mechanical Engineering, The University of Hong Kong, Pokfulam Road, Hong Kong SAR, China*

[e] *Ruđer Bošković Institute, Bijenička 54, 10000 Zagreb, Croatia*

Corresponding Author:
Email: dalek@hku.hk

Experimental Methods

Materials

N,N-dimethylformamide (DMF, anhydrous, 99.9%) was purchased from Thermo Fisher Scientific, dimethyl sulfoxide (DMSO, anhydrous, 99.9%) was purchased from Alfa Aesar. Chlorobenzene (anhydrous, 99.8%) was purchased from Sigma-Aldrich. Lead bromide ($PbBr_2$, ≥98%), lead iodide (PbI_2, ≥98%), (2-(9H-carbazol-9-yl)ethyl)phosphonic acid (2PACz, >98.0%) and (4-(3,6-Dimethyl-9H-carbazol-9-yl)butyl)phosphonic acid (Me4PACz, >98.0%) were purchased from Tokyo Chemical Industry Co., Ltd. (TCI). Methylammoniumn iodide (MAI), Methylammoniumn bromide and phenethylammonium iodide (PEAI) were purchased from Greatcell Solar. [6,6]-phenyl-C_{61}-butyric acid methyl ester (PCBM) and 2,9-Dimethyl-4,7-diphenyl-1,10-phenanthroline (BCP) were purchased from Lumtec. The transparent Indium doped tin oxide (ITO) substrates were sourced from Liaoning YouXuan Technology Co., Ltd. All materials were used as received.

Device fabrication

The ITO substrates were cleaned by detergent, de-ionized (DI) water, Acetone and Ethanol for 30 minutes in sequence. The cleaned substrates were furtherly cleaned by oxygen plasma for 1 min. NiO_x nanoparticles dispersion was prepared by mixing NiO_x nanoparticle powder into DI water with a concentration of 20 mg/mL. The method of synthesizing NiO_x nanoparticle is the same as in our previous work.[1] The NiO_x ink were then spin-coated onto ITO substrate at 4000 rpm for 30 s, followed by a post annealing at 110 °C. The substrates were then transferred into Ar-filled glovebox for deposition of perovskite.

$Cs_{0.03}(FA_{0.83}MA_{0.17})_{0.97}Pb(I_{0.83}Br_{0.17})_3$ (CsFAMA)[1-2]

For CsFAMA perovskite, the precursor was prepared by mixing 18.2 mg CsI, 22.4 mg MABr, 73.4 mg $PbBr_2$, 172 mg FAI and 507.1 mg PbI_2 with 1mL DMF: DMSO (4:1 v:v). The precursor was stirred at 60°C for 1.5 h. Before the deposition of perovskite, 2PACz (0.5mg/mL in IPA) was spin-coated on the top of NiO_x layer at 4000 rpm for 30 s and annealed at 100°C for 10 min. For deposition of perovskite layer, 60 μL of precursor solution was spin-coated at 4000 rpm for 35 s. During the deposition process, 200 μL of Chlorobenzene (CB) was dropped at the 10th second from the beginning of the spin-coating program. The substrate was then annealed at 110 °C for 40 min.

$Cs_{0.05}(FA_{0.98}MA_{0.02})_{0.95}Pb(I_{0.98}Br_{0.02})_3$ (Low-Br)[3]

For Low-Br perovskite, the precursor was prepared by adding 3.7 mg MABr, 19.5 mg CsI, 12 mg $PbBr_2$, 18 mg MACl, 275 mg FAI and 820.7 mg PbI_2 into 1mL DMF: DMSO (8:1 v:v). The precursor was stirred at room temperature for 2 h. Before deposition of perovskite, Me4PACz (0.3 mg/mL in Ethanol) was spin-coated at 4000 rpm for 30s, followed by post-annealing at 100°C for 10 min. 60 μL of precursor were spin-coated at 5000 rpm for 35 s. During the deposition process, 130 μL of CB was dropped at the 15th second before the end of the program. The substrate was then annealed at 80°C for 5 min and 110°C for 20 min.

$Cs_{0.1}FA_{0.9}PbI_{2.9}Br_{0.1}$ (MA-Free)[4]

For MA-Free perovskite, the precursor was prepared by adding 26 mg CsI, 22 mg $PbBr_2$, 155 FAI and 433 mg PbI_2 into mixture of 571 μL DMF and 143 μL DMSO. The precursor was stirred at 50 °C overnight. Before the perovskite deposition, Me4PACz (0.3 mg/mL in Ethanol) was spin-coated at 4000 rpm for 30 s and annealed at 100 °C for 10 min. For perovskite deposition, 60 μL of precursor solution was spin-coated at 2000 rpm for 10 s and 4000 rpm for 30 s sequentially. 220 μL of CB were dropped at the 10th second before the end of the program. The substrate was then annealed at 100 °C for 30 min.

After spin-coating 3D perovskite layer, PEAI (1 mg/mL in IPA) was deposited on the top of perovskite by spin-coating at 5000 rpm for 30 s and annealed at 100°C for 5 min. The method for 2D perovskite deposition was the same for all the 3 kinds of perovskites. To prepare the electron transport layer, PCBM solution (20 mg/mL in CB) was stirred at 60 °C overnight. Then, 60 μL of PCBM solution was spin-coated at 1000 rpm for 30s. The substrate was then annealed at 100 °C for 10 min. After that, BCP solution (0.5 mg/mL in IPA) was spin-coated at 4000 rpm for 30s. No annealing is required afterwards. 100 nm of Ag was deposited by thermal evaporation at the rate of 0.1 Å/s. The active area of the device is 15 mm^2 and limited to 4 mm^2 using a shadow mask for characterization. PIB tape with cover glass was pressed on the top of device at 80 °C for encapsulation. Epoxy resin was used to seal the edge of cover glass for further protection.

Perovskite film characterization

The X-ray diffraction (XRD) diagram was measured by Rigaku MiniFlex 600-C X-ray diffractometer with Cu radiation source. Surface morphology of MA-free perovskite with different additives was examined by Hitachi S-4800 FEG Scanning Electron Microscope. Time-resolved photoluminescence (TRPL) was measured by FLS1000 Photoluminescence Spectrometer (Edinburgh Instruments) with 375 nm laser diode as excitation source operating at 1MHz. The perovskite samples were aged under illumination generated by Sunbrick™ Solar Simulator (G2V) with intensity of 1 sun and AM 1.5G spectrum. Fourier transform infrared spectroscopy (FTIR) measurements were performed using a Bruker Vertex 70v system. The samples for FTIR measurements were prepared by spin-coating, following the same procedure as the perovskite films for device fabrication. For FAI+additive samples, precursor solutions (1.3M in DMF: DMSO=4:1) were spin-coated at 3000 rpm for 35 s, followed by annealing at 100°C.

Device characterization

J-V curve of all the solar cell devices was measured by Keithley 2400 source measure unit controlled by home-made LabView Program. The measurement was conducted under 1 sun (calibrated by Enli PVM silicon standard reference cell), AM 1.5G illumination (ABET Sun 2000) in ambient environment at room temperature. The J-V curves were scanned through forward (-0.2 to 1.2 V) and reverse (1.2 to -0.2 V) with step size of 0.03 mV and delay time of 10 ms. The EQE spectrum of device were measured by QE-R 3011 EQE system (Enli Technology Co. Ltd., Taiwan) with 210 Hz chopped monochromatic light with a range of 300 nm to 900 nm. The open circuit stability of devices was tracked by periodically J-V scan conducted by Puri I-V testing system in ambient environment at room temperature without encapsulation. The Maximum Power Point Traking (MPPT) testing of encapsulated devices was conducted by InfinityPV 8 Channel MPPT testing system at room temperature. All the stability tests were conducted under illumination generated by Sunbrick™ Solar Simulator (G2V). The Pb:I ratio of fresh and aged samples was determined by energy dispersive X-ray (EDX) spectroscopy using a Hitachi Regulus 8230 SEM with a Oxford Ultim Max 170 EDS detector. For samples before aging, the silver electrode was removed right after thermal deposition while for the after group, while for sample after aging electrode was removed after aging in ambient environment (humidity~60%) under illumination with intensity of 1 sun. The PCBM on all the samples was washed off by dynamic spin-coating of chlorobenzene. The EDX spectrum was measured at active area previously covered by the silver electrode.

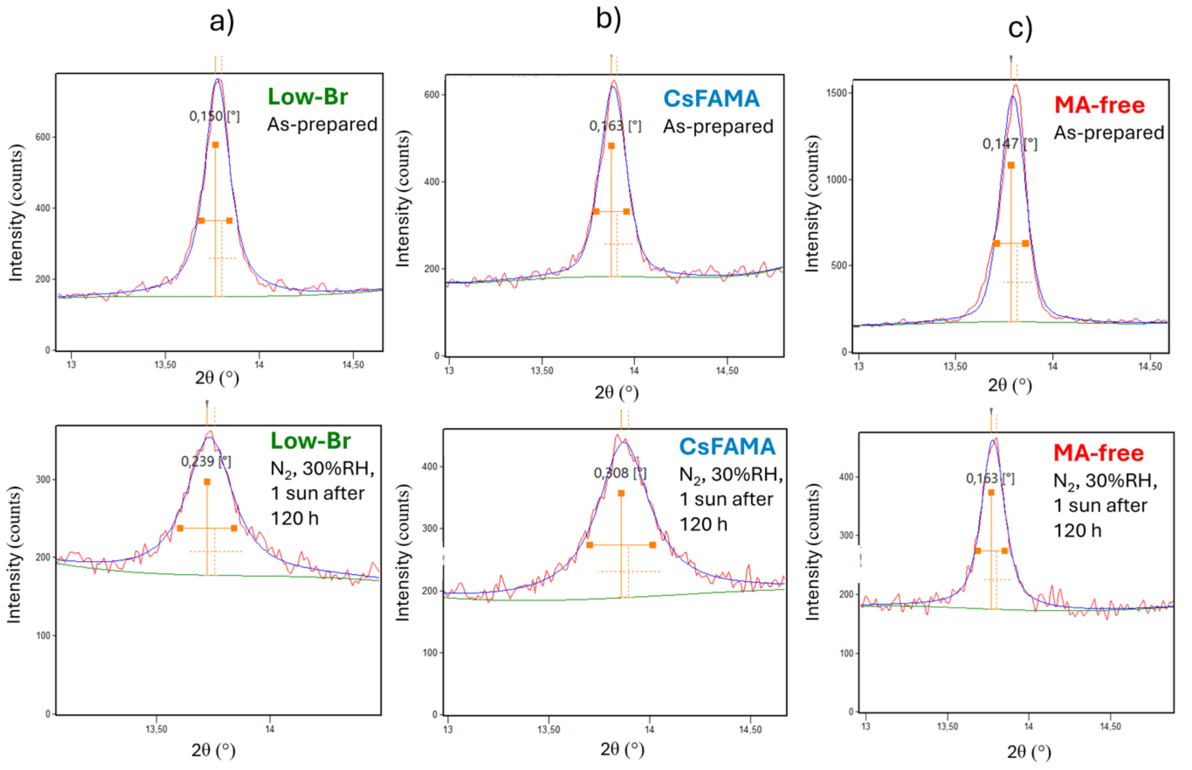

Figure S1. Full-width-at-half-maxima parameter for the 001 diffraction line before and after illumination in N_2 in the presence of moisture for a) low-Br perovskite, b) mixed perovskite c) MA-free perovskite.

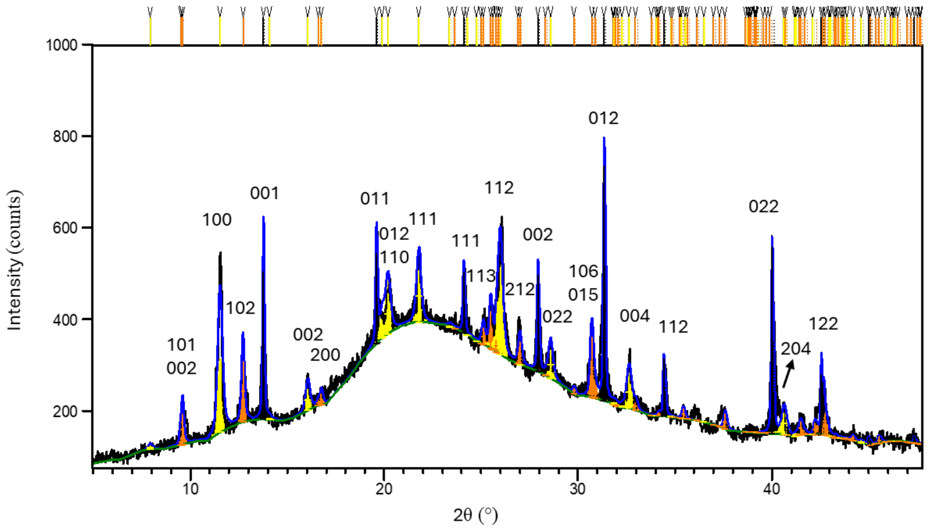

Figure S2. XRD of MA-free perovskite after aging under illumination the N_2 in the presence of moisture. Experimental data are shown as black line while the calculated pattern in given as blue line. Positions of reflections belonging to cubic MA-free are colored black while hexagonal δ-(FA)PbI_3 and orthorhombic δ-$CsPbI_3$ phases are colored in yellow and orange, respectively.

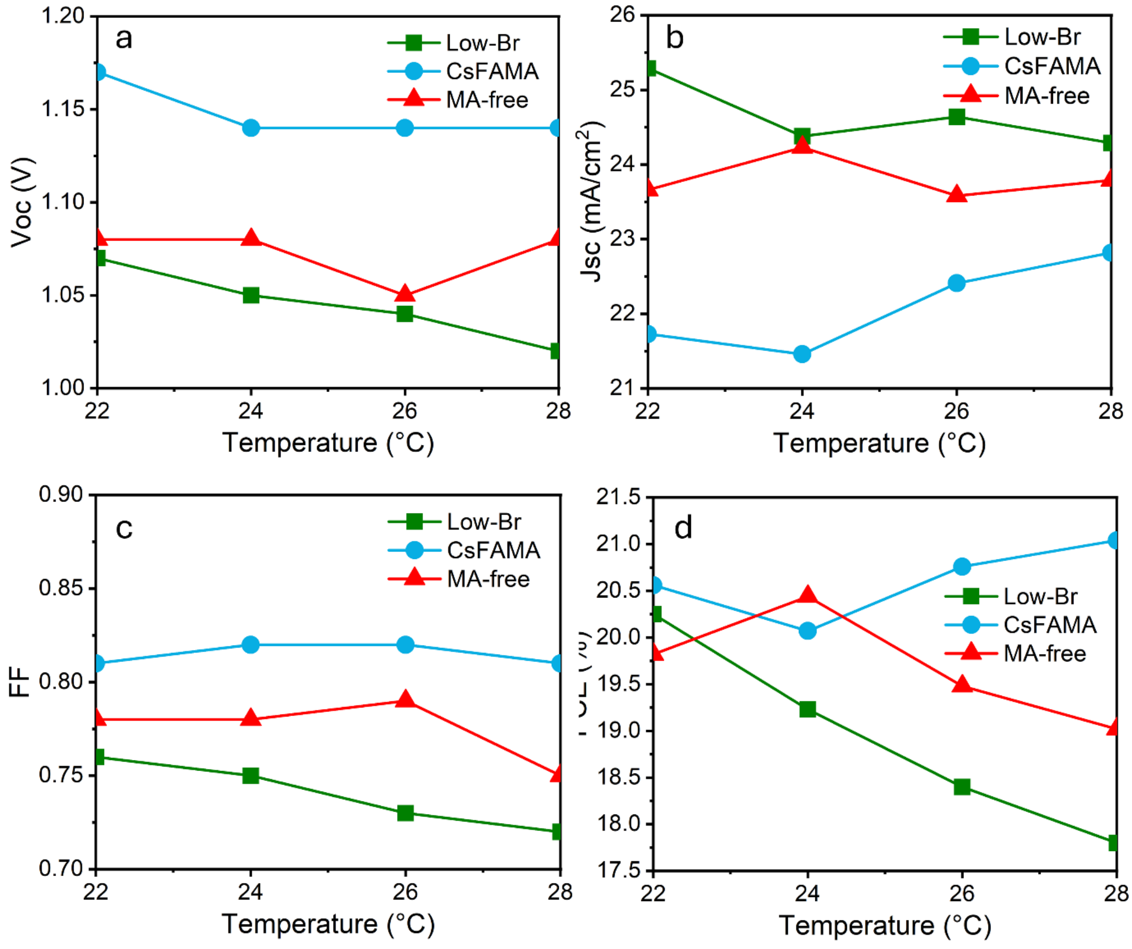

Figure S3. Solar cell performance parameters as a function of glove box temperature. Squares denote Low-Br, circles denote CsFAMA, trangles denote MA-free. a) V_{oc} b) J_{sc} c) FF and d) PCE. Data are shown for reverse scan for champion devices, with the following HTLs: NiO_x+MeO-2PACz for low-Br, and 2PACz for CsFAMA and MA-free.

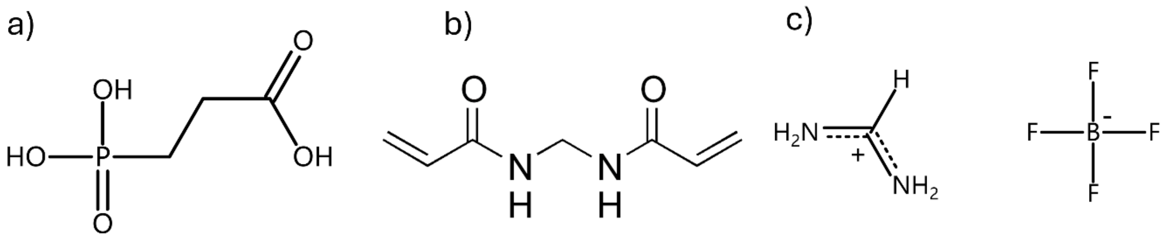

Figure S4. Chemical structures of a) 3-phosphonopropionic acid (3PPA) b) N,N'-methylenebisacrylamide (CL) and c) $FABF_4$.

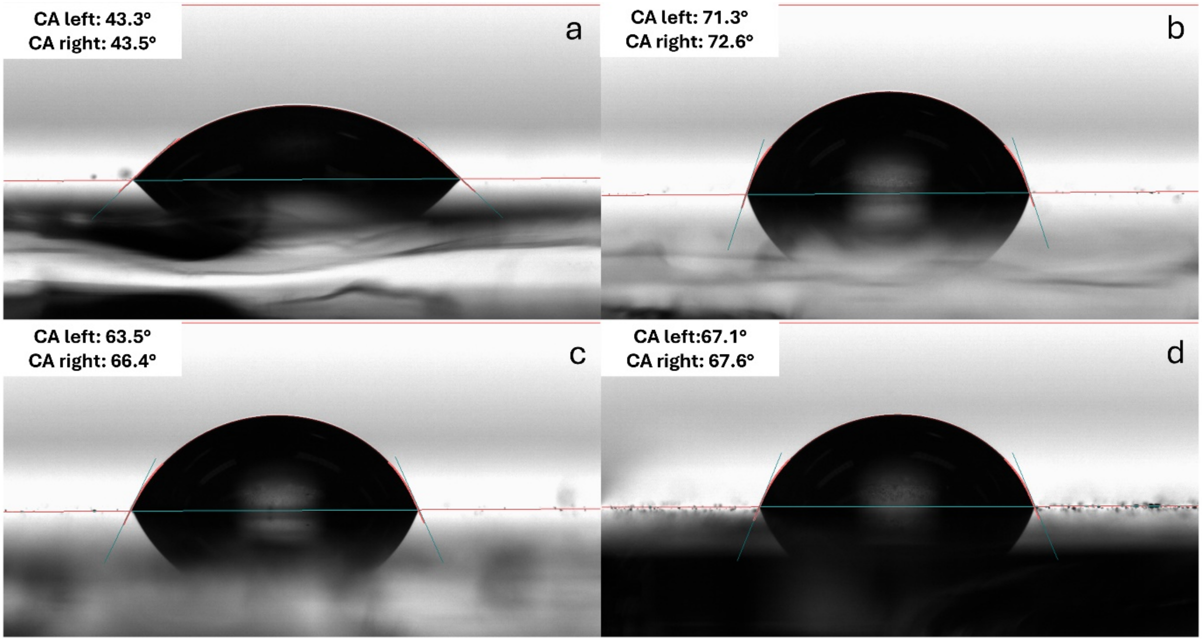

Figure S5.. Contact angle images of perovskite films with different additives a) control b) 3PPA c) $FABF_4$ and d) CL.

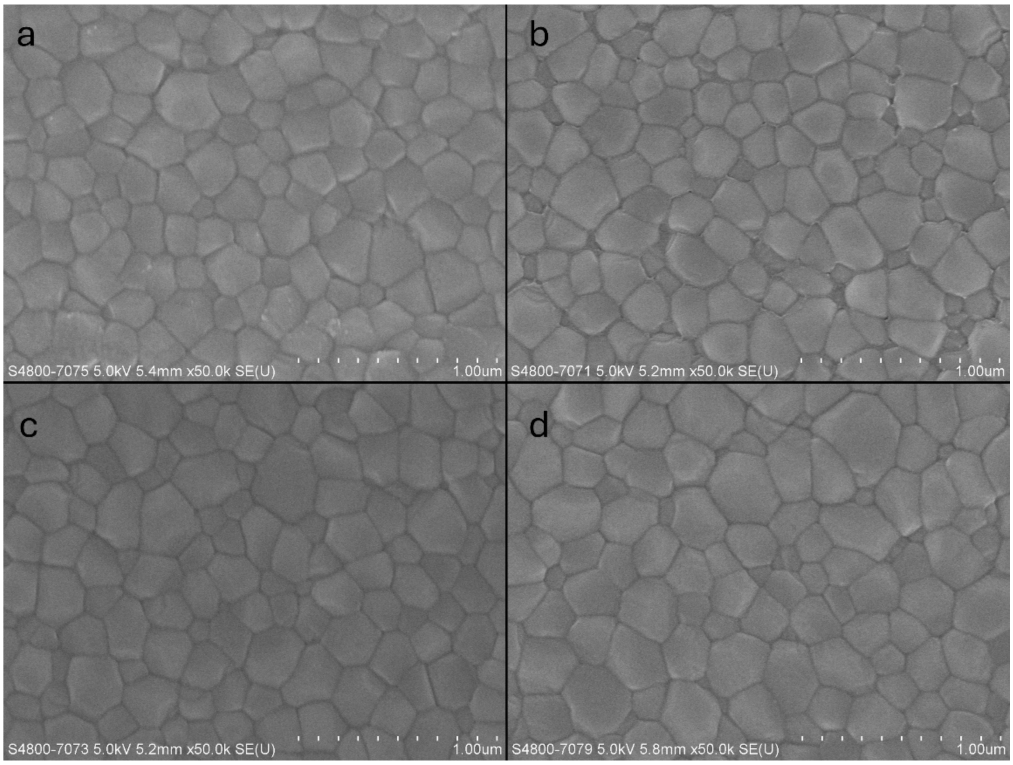

Figure S6. SEM images of perovskite films with different additives a) control b) 3PPA c) $FABF_4$ and d) CL.

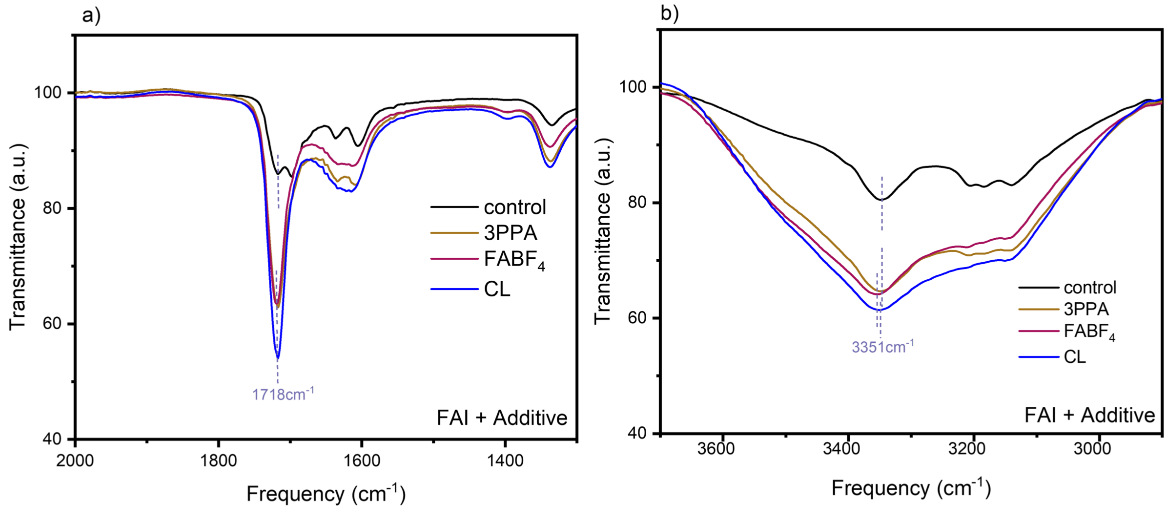

Figure S7. FTIR spectra of FAI+additive films in spectral ranges a) 1300-2000 cm^{-1} and b) 2900-3700 cm^{-1}.

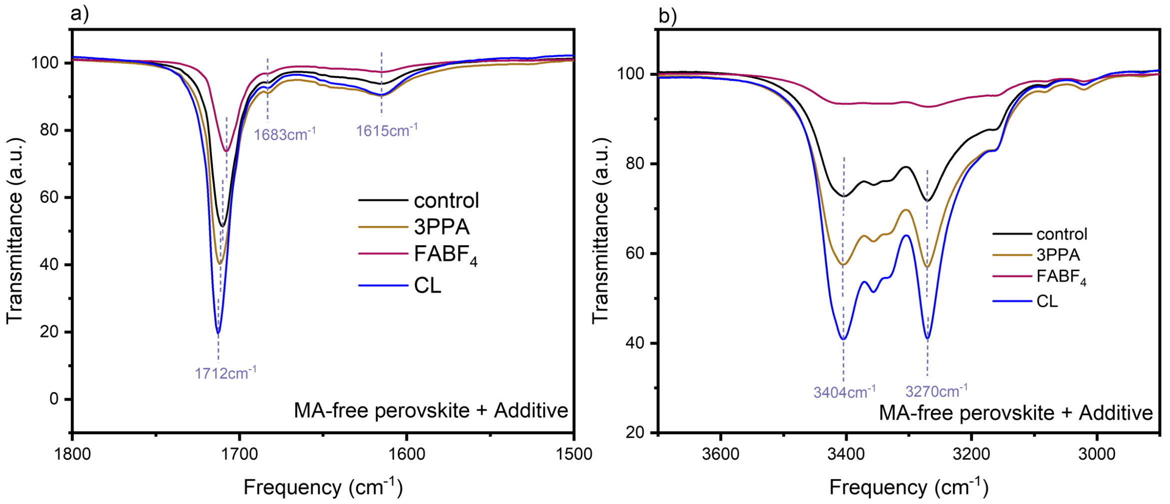

Figure S8. FTIR spectra of MA-free perovskite+additive films in spectral ranges a) 1300-2000 cm^{-1} and b) 2900-3700 cm^{-1}.

Table S1. Fitting parameters for TRPL decay curves for different additives using a bi-exponential decay equation $I(t) = A_1 e^{-t/t_1} + A_2 e^{-t/t_2}$.

Sample	A_1	t_1(ns)	A_2	t_2 (ns)	t_{avg} (ns)
Control	0.39	18.49	0.61	159.41	104.45
3PPA	0.34	0.89	0.66	393.01	259.69
$FABF_4$	0.35	7.10	0.65	225.32	148.94
CL	0.32	0.44	0.68	443.27	301.56

Table S2. Fitting parameters for TRPL decay curves for different additives using a Bimolecular-trapping-detrapping model.[5] B denotes Bimolecular and T denotes trapping percentages in overall recombination, respectively.

Sample	k_B (cm^3/ns)	B (%)	k_T(cm^3/ns)	T (%)	N_T (cm^{-3})	k_D(cm^3/ns)
Control	8.50×10^{-20}	57.48	1.93×10^{-16}	42.52	1.20×10^{14}	3.21×10^{-21}
3PPA	9.49×10^{-20}	63.63	4.48×10^{-15}	36.37	1.02×10^{14}	3.80×10^{-22}
$FABF_4$	3.84×10^{-20}	65.23	5.65×10^{-16}	34.77	1.03×10^{14}	1.23×10^{-18}
CL	3.74×10^{-19}	63.00	9.05×10^{-15}	36.98	9.55×10^{13}	9.08×10^{-21}

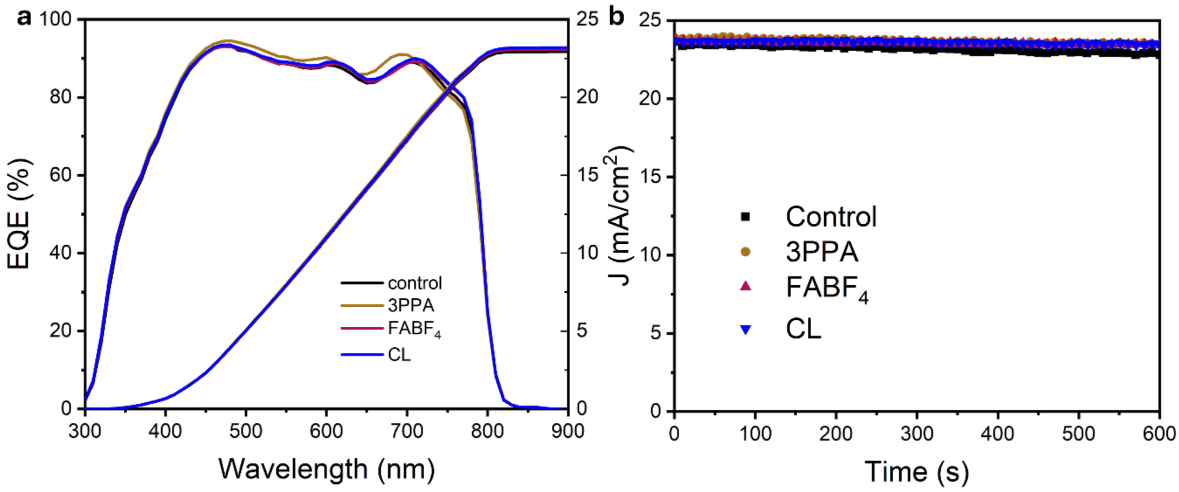

Figure S9.a) External quantum efficiency (EQE) and b) Stabilized power output (SPO) of for perovskite solar cells with different additives. Integrated value of J_{sc} is also indicated in EQE plot.

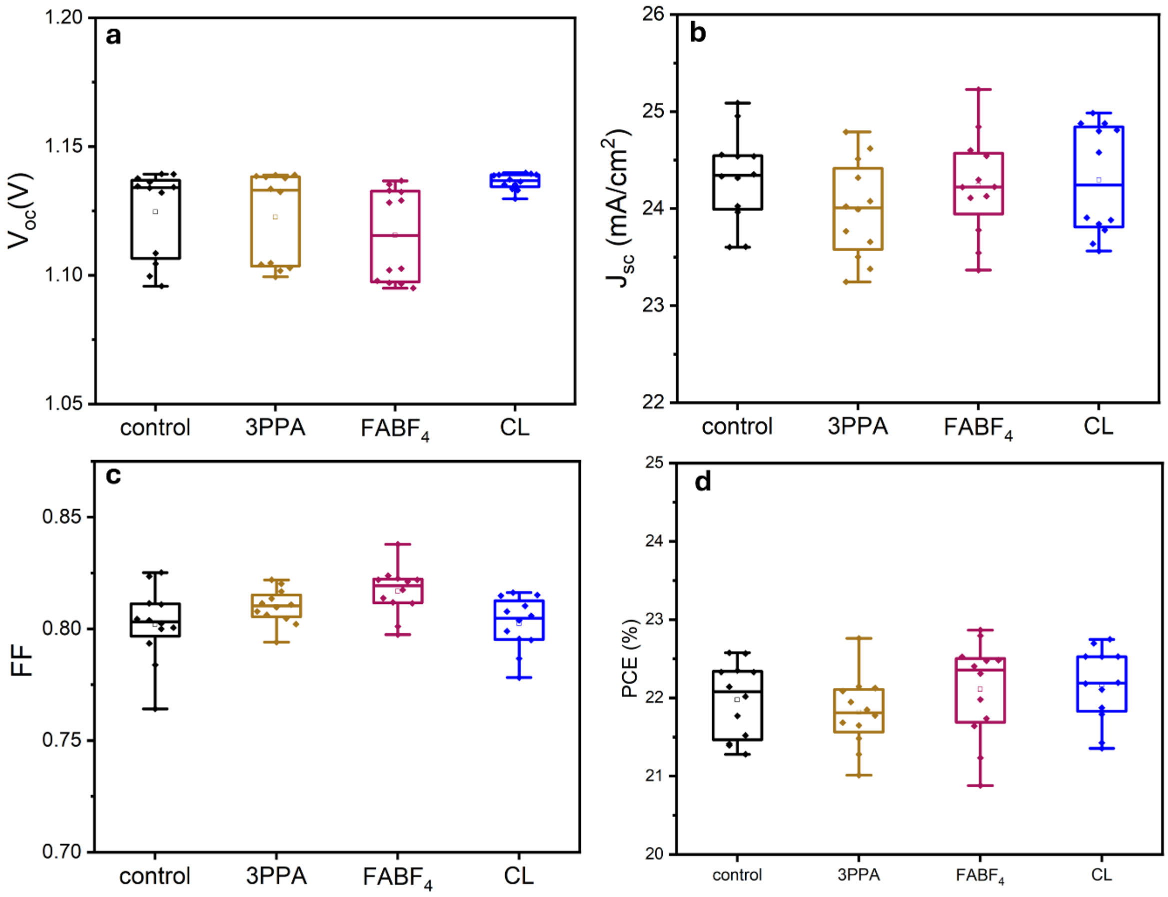

Figure S10. Device performance statistics of solar cells with different additives a) V_{oc} b) J_{sc} c) FF and d) PCE.

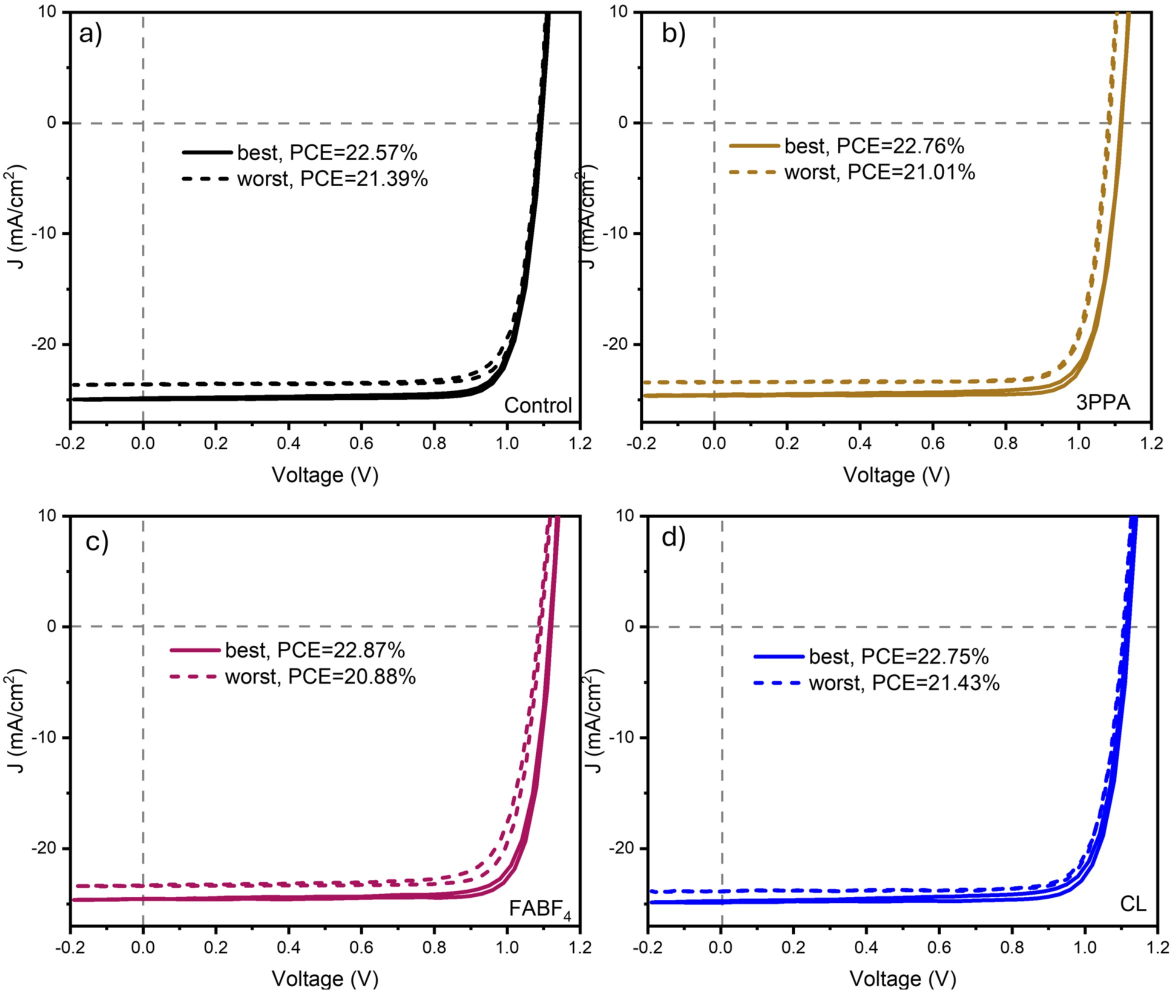

Figure S11. J-V curves of the best and the worst devices for a) Control b) 3PPA c) $FABF_4$ and d) CL.

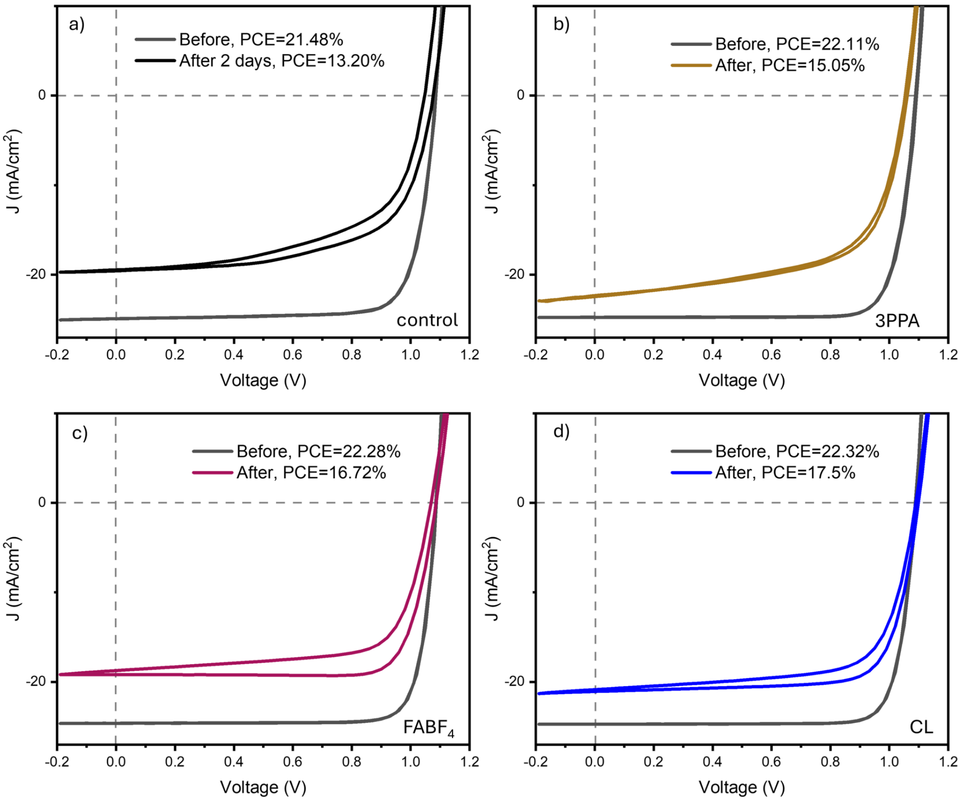

Figure S12. Representative J-V curves before and after aging in ambient (RH ~60%) under open circuit condition and 1 Sun illumination for a) Control b) 3PPA c) FABF$_4$ and d) CL. Aging time was 48 h for Control, and 72 h for different additives, due to faster performance degradation of Control devices.

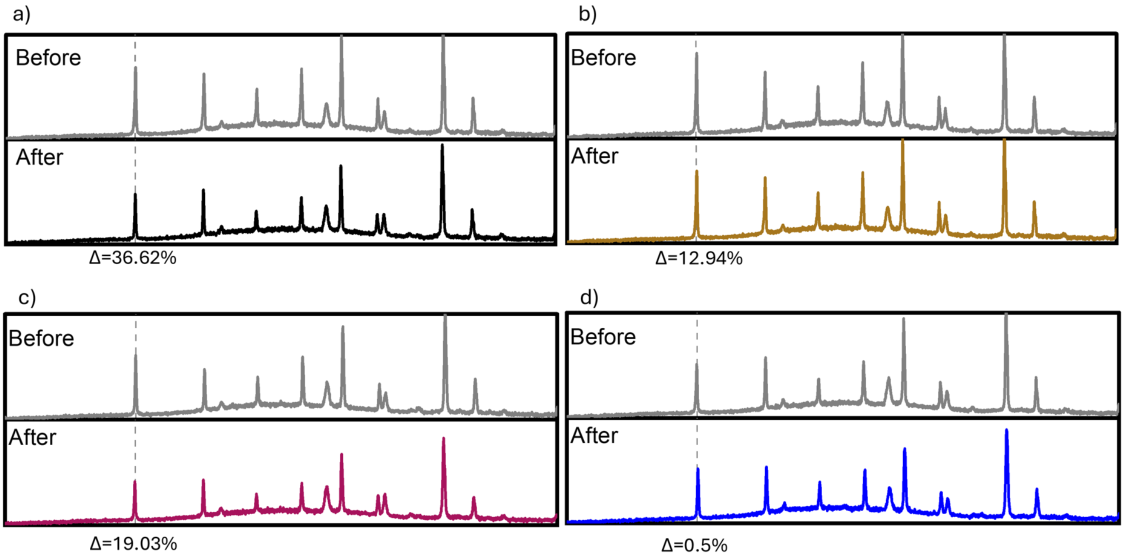

Figure S13. XRD patterns before and after 72 h of aging in ambient (RH ~60%) under open circuit condition and 1 Sun illumination for a) Control b) 3PPA c) FABF$_4$ and d) CL. Δ values were calculated as difference in peak intensities before and after aging, divided by peak intensity after aging.

Table S3. Solar cell performance parameters of solar cells with different perovskite layer. The performance parameters of champion cells are in bold font. Average values are obtained from 12 devices (4 substrates).

Sample name/bias	**J_{sc} (mA/cm^2)**	**V_{oc} (V)**	**FF**	**PCE(%)**
Control-Reverse	24.30±0.36 **24.95**	1.124±0.016 **1.096**	0.802±0.012 **0.825**	21.93±0.42 **22.57**
Control-Forward	24.25±0.37 **24.86**	1.118±0.009 **1.125**	0.791±0.014 **0.793**	21.54±0.51 **22.18**
3PPA-Reverse	23.93±0.38 **24.62**	1.122±0.017 **1.132**	0.810±0.006 **0.817**	21.73±0.28 **22.76**
3PPA-Forward	23.89±0.37 **24.56**	1.068±0.013 **1.115**	0.833±0.014 **0.810**	21.31±0.32 **22.18**
FABF$_4$-Reverse	24.21±0.39 **24.54**	1.114±0.017 **1.129**	0.816±0.008 **0.825**	22.04±0.50 **22.87**
FABF$_4$-Forward	24.12±0.32 **24.54**	1.076±0.016 **1.113**	0.812±0.020 **0.815**	21.16±0.62 **22.27**
CL-Reverse	24.29±0.53 **24.88**	1.136±0.003 **1.130**	0.802±0.010 **0.809**	22.16±0.38 **22.75**
CL-Forward	24.25±0.50 **24.74**	1.125±0.003 **1.116**	0.795±0.010 **0.799**	21.74±0.32 **22.06**

Table S4. EDX characterization of perovskite composition before and after aging in ambient under illumination.

	Element	Atomic (%)	Wt (%)	change in Pb:I ratio (%)
control (before)	Pb	19.19	27.94	2.55
	I	80.81	72.06	
control (after)	Pb	19.68	28.57	
	I	80.32	71.43	
3PPA (before)	Pb	19.34	28.13	1.65
	I	80.66	71.87	
3PPA (after)	Pb	19.66	28.55	
	I	80.34	71.45	
$FABF_4$ (before)	Pb	19.58	28.44	2.09
	I	80.42	71.56	
$FABF_4$ (after)	Pb	19.65	28.53	
	I	80.35	71.47	
CL (before)	Pb	19.32	28.1	0.41
	I	80.68	71.9	
CL (after)	Pb	19.4	28.21	
	I	80.6	71.79	

REFERENCES

1. J. Lin, Y. Wang, A. Khaleed, A. A. Syed, Y. He, C. C. Chan, Y. Li, K. Liu, G. Li, K. S. Wong, *ACS Appl. Mater. Interfaces* **2023**, 15, 24437.
2. a)W. Chen, Y. Zhu, J. Xiu, G. Chen, H. Liang, S. Liu, H. Xue, E. Birgersson, J. W. Ho, X. Qin, *Nat. Energy* **2022**, 7, 229; b)Y. Wang, J. Lin, Y. He, Y. Zhang, Q. Liang, F. Liu, Z. Zhou, C. C. Chan, G. Li, S.-P. Feng, *Solar RRL* **2022**, 6, 2200224.
3. D. Li, Y. Huang, R. Ma, H. Liu, Q. Liang, Y. Han, Z. Ren, K. Liu, P. W. K. Fong, Z. Zhang, *Adv. Energy Mater.* **2023**, 13, 2204247.
4. Q. An, L. Vieler, K. P. Goetz, O. Telschow, Y. J. Hofstetter, R. Buschbeck, A. D. Taylor, Y. Vaynzof, *Adv. Energy Sustainability Res.* **2021**, 2, 2100061.
5. E. V. Péan, S. Dimitrov, C. S. De Castro, M. L. Davies, *Phys. Chem. Chem. Phys.* **2020**, *22*, 28345-28358.